Symmetry **2010**, *2*, 1156-1179: doi:10.3390/sym2021156

OPEN ACCESS

symmetry

ISSN 2073-8994

www.mdpi.com/journal/symmetry

Review

A Critical Assessment of the Performance of Magnetic and Electronic Indices of Aromaticity

Miquel Solà [1,*], Ferran Feixas [1], J. Oscar C. Jiménez-Halla [1], Eduard Matito [2,*] and Jordi Poater [1,*]

[1] Institut de Química Computacional and Departament de Química, Universitat de Girona, Campus de Montilivi, 17071 Girona, Catalonia, Spain; E-Mails: ferran.feixas@udg.edu (F.F.); oscar@stark.udg.edu (J.O.C.J.H.)

[2] Institute of Physics, University of Szczecin, 70-451 Szczecin, Poland

* Authors to whom correspondence should be addressed; E-Mails: miquel.sola@udg.edu (M.S.); ematito@gmail.com (E.M.); jordi.poater@udg.edu (J.P.).

Received: 17 February 2010; in revised form: 7 May 2010 / Accepted: 10 June 2010 / Published: 14 June 2010

Abstract: The lack of reference aromatic systems in the realm of inorganic aromatic compounds makes the evaluation of aromaticity in all-metal and semimetal clusters a difficult task. To date, calculation of nucleus-independent chemical shifts (NICS) has been the most widely used method to discuss aromaticity in these systems. In the first part of this work, we briefly review our previous studies, showing some pitfalls of the NICS indicator of aromaticity in organic molecules. Then, we refer to our study on the performance of some aromaticity indices in a series of 15 aromaticity tests, which can be used to analyze the advantages and drawbacks of aromaticity descriptors. It is shown that indices based on the study of electron delocalization are the most accurate among those analyzed in the series of proposed tests, while $NICS(1)_{zz}$ and $NICS(0)_{\pi zz}$ present the best behavior among NICS indices. In the second part, we discuss the use of NICS and electronic multicenter indices (MCI) in inorganic clusters. In particular, we evaluate the aromaticity of two series of all-metal and semimetal clusters with predictable aromaticity trends by means of NICS and MCI. Results show that the expected trends are generally better reproduced by MCI than NICS. It is concluded that $NICS(0)_{\pi}$ and $NICS(0)_{\pi zz}$ are the kind of NICS that perform the best among the different NICS indices analyzed for the studied series of inorganic compounds.

Keywords: Aromaticity; inorganic clusters; DFT calculations; nucleus-independent chemical shifts; multicenter electronic indices

1. Introduction

Originally, the concept of aromaticity was introduced to rationalize the structure, stability, and reactivity of benzene and related organic compounds. However, in the last decades, the boundaries of aromaticity have been extended to new areas of chemistry and to a large list of highly diverse species, which were unimaginable some decades ago [1,2]. The proliferation of new aromatic compounds compelled to reconsider the traditional definition based on the Hückel's $(4n + 2)\pi$ electrons rule. Thus, species considered as Möbius aromatic [3,4] disobeyed the $(4n + 2)\pi$ electrons rule while spherical aromatic compounds such as certain fullerenes added a third dimension to aromaticity [5,6]. Both descriptions broke down the well-established relation between aromaticity and planarity. Moreover, metalloaromaticity [7] opened the way to organometallic and inorganic aromatic species and the discovery of σ-aromaticity [8–10] demonstrated that, in some cases, the contribution of the σ orbitals is crucial to explain the high electron delocalization. Consequently, the definition and limits of aromaticity have been constantly updated in order to take into account the whole spectrum of new aromatic compounds. Nowadays, the concept of aromaticity can be used to explain structure, stability, and reactivity not only of classical organic compounds but also of many organometallic and inorganic species, in particular, of all-metal and semimetal clusters.

Clusters serve as a link between the atom and the bulk material. They exhibit characteristics of both forms of matter, depending on their size and their particular molecular and electronic structures. The properties of such molecules make them potentially useful for technical applications such as specific and very efficient catalysts, drugs, and other novel materials with as yet unimagined features. Recently discovered [11], all-metal and semimetal aromatic clusters represent one of the new boundaries of material science (three recent reviews on this kind of clusters can be found in Refs. [12–14]). The unusual stability of all these clusters comes from their aromatic character. Indeed, the aromaticity is a key property of these compounds since it explains their molecular and electronic structure, stability, and reactivity. At variance with the classical aromatic organic molecules that possess only π-electron delocalization, these compounds present σ-, π-, and δ- (involving d orbitals) [15–17] or even ϕ-(involving f orbitals) [18] electron delocalization, exhibiting characteristics of what has been called multifold aromaticity [12–14,19–22].

An in-depth analysis of all-metal and semimetal clusters requires evaluation of their aromaticity. This evaluation is not unique since a plethora of different measures based on structural- [23,24], magnetic- [25], energetic- [26], and electronic-based [27,28] indices can be used to quantify aromaticity of a given set of compounds. In many cases, results obtained from different indicators of aromaticity may reveal contradictory trends [29], which complicates matters. In addition, principal component analyses suggest that aromaticity has multidimensional character [30–33]. Consequently, aromatic compounds cannot normally be well-characterized by using a unique index and, in order to make reliable comparisons, it is usually recommended to employ several aromaticity descriptors [25,27,29]. Unfortunately, in the case of inorganic clusters only few indices can provide reliable measures of aromaticity. The reason being that most of the current available methods to quantify aromaticity have been designed to measure the aromaticity of classical aromatic organic molecules; they cannot be applied directly to inorganic clusters without additional adjustments. Thus, the harmonic oscillator model of aromaticity (HOMA) [34,35], the most widely used geometry-based

indicator of aromaticity, takes benzene, the archetype aromatic molecule, or other aromatic organic molecules, as a reference in its definition. Similarly, the electronic-based descriptors such as the aromatic fluctuation (FLU) [36] indicator of aromaticity, the bond order index of aromaticity (BOIA) [37], or the aromaticity index θ proposed by Matta and Hernández-Trujillo [38,39] use references obtained from organic aromatic compounds in their definitions and they cannot be used in inorganic species without redefining the reference values. Likewise, energetic-based indicators such as resonance energies (RE) or aromatic stabilization energies (ASE) [26] are difficult to compute accurately in all-metal clusters because of their lack of appropriate reference systems [19,40]. Since there are no inorganic species characterized as fully aromatic and capable of serving as an inorganic reference system, it is not yet possible to derive a comparative scale as in organic chemistry. For the moment, the most widely used methods to discuss aromaticity in inorganic clusters are the basic electron counting based on the 4n + 2 Hückel's rule [41–44] and the magnetic-based indicators of aromaticity, in particular, the nucleus-independent chemical shifts (NICS) [45]. In some cases, electronic multicenter indices (MCI) [37,46-49] have also been used [50–52].

The 4n + 2 rule, according to which a monocyclic system with (4n + 2π)-electrons is aromatic while a system with 4nπ-electrons is antiaromatic, offers the easiest assessment of aromaticity. However, simple total electronic counts lead sometimes to incorrect results [14,53–55]. In addition, electron counting does not provide a quantitative value, so comparisons of aromaticity from different compounds are not possible.

Until now, the most widely employed method to analyze the aromaticity of all-metal and semimetal species is the NICS index [18,56–61]. This magnetic-based descriptor of aromaticity was introduced by Schleyer and co-workers [45]. It is defined as the negative value of the absolute shielding computed at a ring center or at some other point, usually at 1 Å above the ring center. Rings with large negative NICS values are considered aromatic, whereas rings with positive NICS values are regarded as antiaromatic. This has many advantages among other indicators of aromaticity. First, it is a very accessible and easy to compute descriptor; second, it can be used to discuss both the local and the global aromaticity of molecules, and, third, it does not use reference values, so it can be easily applied to any molecule. However, it is not free from criticism. Lazzeretti [62,63] and Aihara [64] have pointed out in several works that NICS's validity to indicate diamagnetic ring currents is limited by the potential spurious contributions from the in-plane tensor components that, at least in classical organic aromatic compounds, are not related to aromaticity. This effect is partially avoided by using NICS(1), that is considered to better reflect the π-electron effects [65–68], or with its corresponding out-of-plane tensor component ($NICS(1)_{zz}$) or even better with the π contribution to this component computed at the ring center or at 1 Å above ($NICS(0)_{\pi zz}$ and $NICS(1)_{\pi zz}$, respectively). In 1997, the first dissected NICS were introduced by Schleyer *et al.* [68] and were applied to study the aromaticity of some inorganic rings. $NICS_{\pi}$ values can be calculated through the decomposition of NICS indices into their canonical molecular orbital (CMO) components [69] using the NBO 5.0 program [70,71]. $NICS(1)_{zz}$ and $NICS(0)_{\pi zz}$ were reported to be the best measures of aromaticity among the different NICS-related definitions in organic molecules [66,72,73]. Other problems that can be found are related to ring size dependence of NICS values [74]. Last but not least, the coupling of magnetic fields from different regions of the molecule can have a large influence on the NICS value of a given ring. This latter aspect is discussed in detail in the next section.

Less common is the use of electronic multicenter indices to study multifold aromaticity in inorganic species. MCI is a particular extension of the I_{ring} index [46].

$$I_{ring}(\mathcal{A}) = \sum_{i_1,i_2,\cdots,i_N} n_{i_1} \cdots n_{i_N} S_{i_1 i_2}(A_1) S_{i_2 i_3}(A_2) \cdots S_{i_N i_1}(A_N) \tag{1}$$

n_i being the occupancy of MO i and $S_{ij}(A)$ the overlap between MOs i and j within the molecular space assigned to atom A. Summing up all the I_{ring} values resulting from the permutations of indices A_1, A_2, ..., A_N the mentioned MCI index is defined as [37,47]:

$$MCI(\mathcal{A}) = \frac{1}{2N} \sum_{P(\mathcal{A})} I_{ring}(\mathcal{A}) \tag{2}$$

where P(A) stands for a permutation operator which interchanges the atomic labels A_1, A_2, ..., A_N to generate up to the N! permutations of the elements in the string A. MCI and I_{ring} give an idea of the electron sharing between all atoms in the ring. The more positive the MCI values, the more aromatic the rings. For planar species, $S_{\sigma\pi}(A) = 0$ and MCI can be exactly split into the σ- and π-contributions in order to obtain MCI_σ and MCI_π. This feature is especially interesting to evaluate multifold aromaticity in all-metal clusters.

2. Some Reported NICS Drawbacks

In the work of Reference [75], where the para-delocalization index (PDI) index was introduced as a new electronic aromaticity criterion, we found that for some six-membered rings (6-MRs) there was a bad correlation between NICS and PDI values. For instance, in anthracene and naphthacene the aromaticity attributed by NICS and PDI to the central as compared to the external ring was very different. Similarly, the aromaticity of the 6-MR of benzocyclobutadiene and biphenylene and that of the 6-MR of pyracylene calculated with NICS and PDI did not correlate. These divergences were attributed to the effect of the currents of adjacent rings where NICS is calculated, causing, for instance, an overestimation of the aromaticity of the central rings of polyacenes [24,64,76,77], or an underestimation for the 6-MRs in contact with nonaromatic and paratropic 4- and 5-MRs. To prove the hypothesis of a possible underestimation by NICS of the aromaticity of the 6-MR in pyracylene, we analyzed [78] the effect of pyracylene pyramidalization, by imposing angles of θ degrees [79] between the planes defined by the rings (see Figure 1), on NICS, HOMA, and PDI indices, and ring currents.

Table 1 lists the values obtained from local (HOMA, NICS, and PDI) aromaticity criteria for the 6-MR of the different pyramidalized pyracylenes. With respect to PDI, there is a small reduction of local aromaticity with an increase of the angle of distortion, in agreement with previous experimental [80-84] and theoretical results [85–88] on distorted aromatic rings. HOMA yields a similar trend with a slight deviation for θ = 10 and 20º. On the other hand, unexpectedly, the local NICS(0) magnetic-based measure shows a steady increase of aromaticity with the distortion of pyracylene.

Figure 1. Schematic representation of (a) pyracylene, (b) how pyracylene has been pyramidalized and (c) the final result for θ = 30º. Reprinted from Reference [78]. Copyright 2004 American Chemical Society.

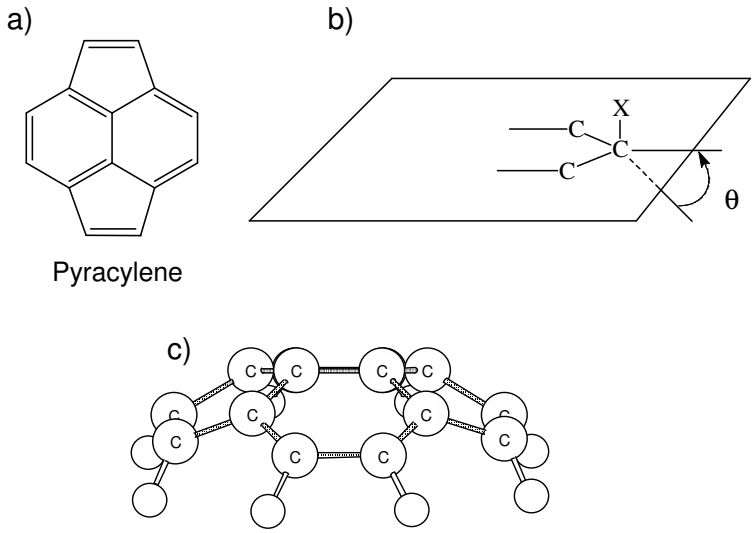

Table 1. θ angle (degrees), PDI (electrons) and HOMA indices, and NICS(0), $NICS(1)_{in}$, and $NICS(1)_{out}$ values at hexagons (ppm) for the different distorted pyracylene molecules (as shown in Figure 1) optimized at the B3LYP/6-31G(d,p) level of theory [a].

θ	PDI	HOMA	NICS(0)	$NICS(1)_{in}$	$NICS(1)_{out}$
0.	0.0675	0.755	−0.1	−2.8	−2.8
10.	0.0672	0.761	−0.1	−3.8	−2.1
20.	0.0666	0.771	−0.6	−5.5	−1.6
30.	0.0656	0.744	−1.7	−7.6	−1.2
40.	0.0646	0.572	−3.7	−9.9	−0.8

[a] From Reference [78]

To get a deeper insight into the origin of the apparent failure of magnetic-based indices of aromaticity for this system, the ring current density maps (at 0.9 a.u. above the ring plane studied) of pyracylene were analyzed [89,90]. For the planar pyracylene, dominant paratropic ring currents circulating on pentagons can be observed, more intense than the diatropic ring current flowing on the naphthalene perimeter (see Figure 2a). However, when increasing the pyramidalization, the diatropic ring current remains quite constant (see Figure 2b), but the paratropic ring current in the pentagonal rings decreases to a breaking point for θ = 40º (see Figure 2c). Moreover, it is also possible to get quantitative information from the ring currents by calculating the magnetic shielding tensors. In particular, the out-of-plane component, σ_{out}, is the negative of the $NICS(0)_{zz}$ value. σ_{out} is –6.2 for the 6-MR of the optimized planar pyracylene, compared with 8.2 for benzene. The unexpected negative value of pyracylene for a diatropic ring can only be attributed to the intense paratropic ring currents on pentagons (σ_{out} = –61.5), thus largely influencing the value for the 6-MRs. When bending, σ_{out} for pentagons becomes less negative, thus σ_{out} for hexagons also increases up to 7.9 for θ = 40º, a value very close to that of benzene. So, these values perfectly corroborate the information already obtained from the ring current density maps.

Figure 2. First-order π-electron current density map calculated with the 6-31G(d,p) basis set using the CTOCD-DZ2 approach at the B3LYP/6-31G(d,p) optimized geometry. The plot plane lies at 0.9 a.u. above the molecular plane. The unitary inducing magnetic field is perpendicular and points outward so that diatropic/paratropic circulations are clockwise/counter clockwise. Representation for (a) planar pyracylene, (b) the distorted θ = 40º pyracylene with the plot plane parallel to a 6-MR ring (in blue), (c) the distorted θ = 40º pyracylene with the plot plane parallel to a 5-MR (blue). The green portion of the molecular frame lies above the plot plane. Reprinted from Reference [78]. Copyright 2004 American Chemical Society.

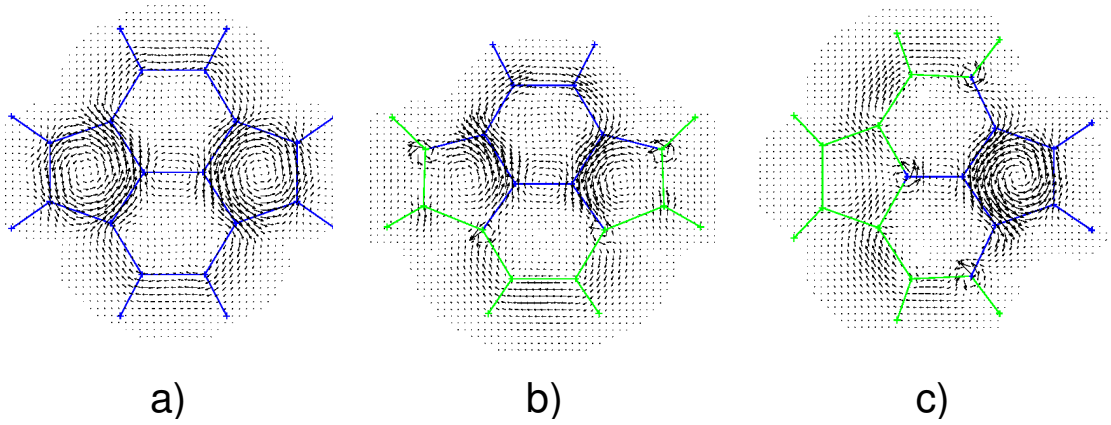

In addition, the NICS at 1 Å above and below the center of the ring ($NICS(1)_{out}$ and $NICS(1)_{in}$, respectively), considered to better reflect the π-electron effects [66,67], have also been calculated for these systems. The values in Table 1 show that NICS(0) and $NICS(1)_{in}$ follow the same trend, thus increasing the aromaticity with bending, however, $NICS(1)_{out}$ follows the expected opposite behavior, like HOMA and PDI. Therefore, it is seen that pyracylene is a problematic case for the NICS indicator of aromaticity, which yields different results depending on where it is calculated. Ring current density maps have proven that aromaticity does not increase with bending. The observed NICS(0) reduction in the 6-MRs of pyracylene upon bending is due to, first, a strong reduction of the paratropic ring current in the adjacent pentagonal rings, and second, to the fact that the effects of paratropic currents point out in other directions.

Magnetic couplings have a significant effect on the measured NICS values also in stacked aromatic rings. In this situation, a considerable reduction of the NICS values in these rings is observed, which indicates an apparent increase in their aromatic character. We showed in a previous work [91] that this decrease is not due to an increase of the electron density in the inner region between the rings, as suggested by some authors [92], but is the result of magnetic couplings between superimposed rings. To prove this we computed the NICS scan for [2.2]paracyclophane with two stacked aromatic rings and we compared it with those of free benzene, *p*-xylene, and benzene dimer that were taken as reference models (see Figure 3). Figure 4 shows the NICS scan obtained when moving along the z-axis in the perpendicular direction to the ring plane for the systems depicted in Figure 3. Positive values of R correspond to the inner region between aromatic rings ($NICS_{in}$), while the outer region ($NICS_{out}$) has negative R values. As compared to free benzene, the benzene dimer has more negative NICS values, especially in the inner region between the two aromatic rings (positive R values). This decrease can be

rationalized from the empirical model of shielding for benzene determined using a current loop model [93]. For [2.2]paracyclophane an additional decrease of NICS in the inner region is observed, while in the outer region NICS increases somewhat. This unexpected increase in the outer region was attributed to the fact that the two aromatic rings in [2.2]paracyclophane are not completely parallel. A similar behavior was found for $NICS_{zz}$ scans. On the other hand, HOMA values suggest a small reduction of aromaticity for the 6-MRs of [2.2]paracyclophane in comparison to free benzene [92]. From these results it is proved that the increase of local aromaticity in superimposed aromatic rings indicated by NICS is not real but the result of the coupling between the magnetic fields generated by the two stacked rings. This result warns about the use of NICS as a descriptor of aromaticity for species having superimposed aromatic rings. We found that these magnetic couplings, *i.e.,* the sum of the magnetic fields created by two superimposed aromatic rings, are also in the origin of the NICS overestimation of aromaticity in helicenes [94,95] and in π-stacked polyfluorenes [96].

Figure 3. A schematic representation of the species analyzed. Reprinted from Reference [91]. Copyright 2006 American Chemical Society.

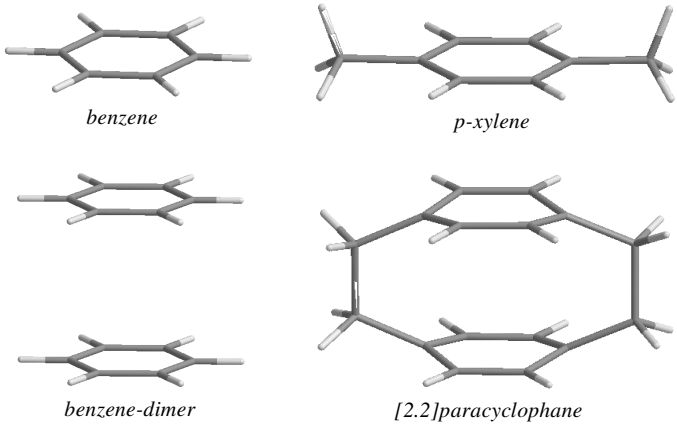

Figure 4. Evolution of NICS obtained at the B3LYP/6-31+G(d,p) level of theory along the z-axis of benzene, p-xylene, benzene dimer, and [2.2]paracyclophane. R represents the distance from the center of the ring; positive R values correspond to $NICS_{in}$ and negative R values correspond to $NICS_{out}$. Reprinted from Reference [91]. Copyright 2006 American Chemical Society.

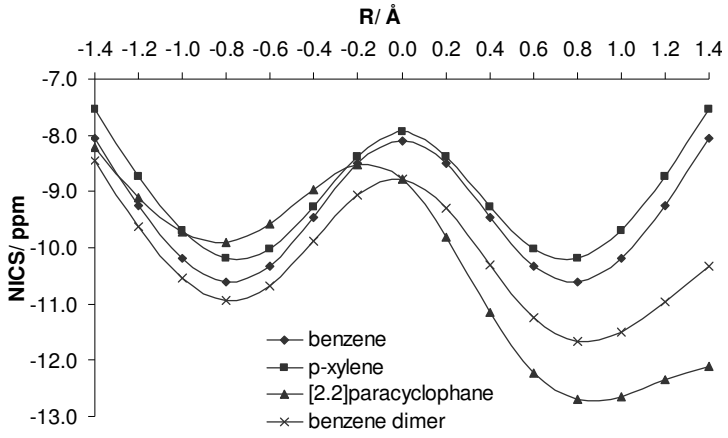

Another interesting example in which certain NICS measures fail, is the case of the benzene ring in the $(\eta^6\text{-}C_6H_6)Cr(CO)_3$ complex. We decided to analyze this system [97] because we were puzzled by the claims of Mitchell and co-workers [98–101] that the benzene ring in tricarbonylchromium-complexed benzene is *ca.* 30–40% more aromatic than benzene itself based on NICS results. It is widely accepted that the structure, reactivity, and aromaticity of the benzene ring are altered significantly upon complexation with the chromium tricarbonyl complex. Thus, after coordination the ring expands, loses its planarity (the hydrogen atoms of the benzene ring slightly bent towards the $Cr(CO)_3$ fragment [102]), and shows an increased difference between alternated short and long C-C bonds [103]. These changes can be rationalized taking into account the nature of the bond between the arene and the metal in (η^6-arene)tricarbonylchromium complexes [104]. The dominant bonding mechanism corresponds to the interaction of the degenerate *2e* LUMO and $2a_1$ LUMO+1 orbitals of the $Cr(CO)_3$ moiety with the highest occupied π-orbitals of the arene with the appropriated symmetry [105]. Charge transfer from the highest occupied π-orbitals of the arene to the lowest unoccupied *2e* and $2a_1$ orbitals of $Cr(CO)_3$ partially breaks the C–C bonds, thus explaining the observed expansion of the aromatic ring and the increase in bond length alternation in the benzene ring of $(\eta^6\text{-}C_6H_6)Cr(CO)_3$. Because of the loss of π electron density in the ring, one should expect a partial disruption of aromaticity in the benzene ring of $(\eta^6\text{-}C_6H_6)Cr(CO)_3$ in comparison to free benzene, as discussed by Hubig *et al.* [103] and not the increase of aromaticity observed by Mitchell and co-workers [98–101]. Indeed, all indices used by us [97], except NICS(0) and NICS(1), showed that there is a clear reduction of the aromaticity of benzene upon coordination to the $Cr(CO)_3$ complex. We analyzed the particular behavior of the NICS index and we concluded that the reduction of the NICS value in the benzene ring of the $(\eta^6\text{-}C_6H_6)Cr(CO)_3$ complex is not a manifestation of an increased aromaticity of the 6-MR but is due to the ring currents generated by the electron pairs that take part in the benzene-$Cr(CO)_3$ bonding [97]. The coupling of the induced magnetic field generated by these electron pairs and that of the aromatic ring leads to an artificial reduction of the NICS(0) and NICS(1) values pointing to a non-existent increase of aromaticity. However, it has to be said that $NICS(1)_{zz}$ index indicates the correct reduction of aromaticity of the benzene ring upon complexation [73].

3. A Critical Assessment of Aromaticity Indices Using a Test Set

Recently, we proposed a series of 15 aromaticity tests (see Scheme 1) that can be used to analyze the advantages and drawbacks of a group of aromaticity descriptors [73]. Exploring the successes and breakdowns of the different aromaticity indices is relevant not only for its own sake but as a way to get ideas of how to improve present indicators of aromaticity and define new indices that correlate better with chemical intuition for most of the well-established cases. For this reason, it is very important, in our opinion, to devise methodologies that allow quantifying the performance of the existing and new defined indices of local aromaticity. To this end, we consider that the use of a set of simple tests that include systems having widely-accepted aromaticity behaviors can be helpful to discuss aromaticity in organic species.

Scheme 1. Schematic representation of the 15 proposed tests. The sign "*" indicates the position where NICS(1) has been calculated. Reprinted from Reference [73]. Copyright 2008 Wiley Periodicals, Inc.

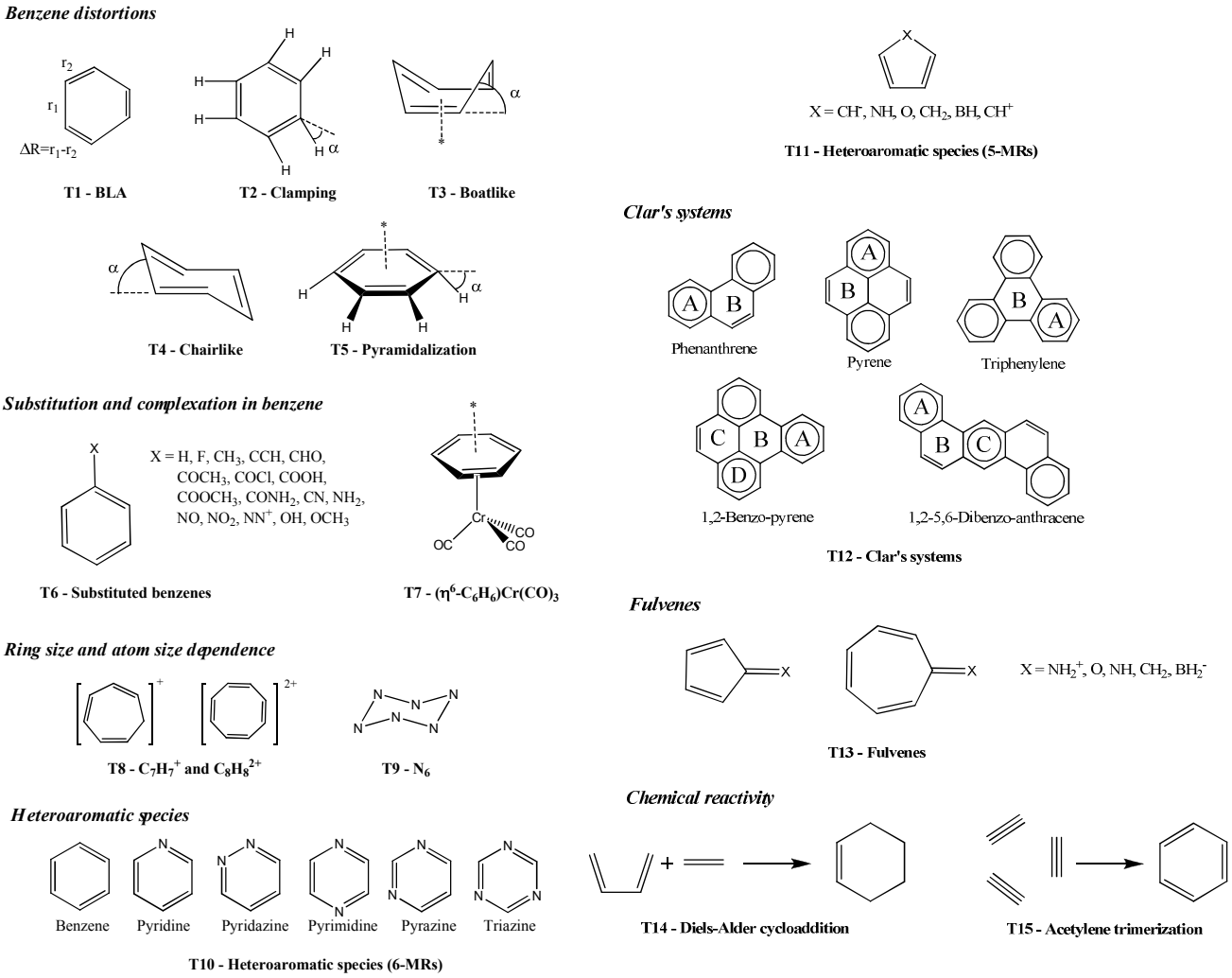

In order to analyze the performance of aromaticity indices in a series of 15 tests, we made a selection of different descriptors of aromaticity based on structural (HOMA), magnetic (NICS(0), NICS(1) and NICS(1)$_{zz}$) and electronic (PDI, FLU, MCI and I_{ring}) manifestations of aromaticity. Table 2 summarizes the results obtained in all tests. We write "yes" when certain indices follow the expected trend in aromaticity for a given test, "no" otherwise, and "unclear" when the failure of the index is minor. Moreover, we have completed Table 2 with the values of NICS(0)$_{\pi}$ and NICS(0)$_{\pi zz}$ which were not analyzed in Reference [73]. Our results indicated that the best indices are the multicenter indices, especially MCI that fails only in the test T10. On the other hand, NICS(1)$_{zz}$ and NICS(0)$_{\pi zz}$ are the kind of NICS that perform the best among the different NICS indices analyzed. These results are in line with a previous study [72] where a set of NICS indices were assessed and compared with aromatic stabilization energies (ASE) of 75 five-membered rings. Since NICS(0)$_{\pi zz}$ was not analyzed in Reference [73] its performance is discussed in the following lines.

Table 2. Summary of the 15 tests applied at the B3LYP/6-311++G(d,p) level for the 10 descriptors of aromaticity analyzed. Data from Reference [73] except for NICS(0)$_\pi$ and NICS(0)$_{\pi zz}$ results.

	PDI	FLU	MCI	I_{ring}	HOMA	NICS(0)	NICS(1)	NICS(1)$_{zz}$	NICS(0)$_\pi$	NICS(0)$_{\pi zz}$
T1	Yes	Yes	Yes	Yes	Unclear[a]	Yes	Yes	Yes	Yes	Yes
T2	Unclear[b]	Yes	Yes	Yes	Unclear[a]	Unclear[c]	Yes	Yes	Unclear[c]	Yes
T3	Unclear[b]	Yes	Yes	Yes	Yes	Yes	Yes	Yes	Yes	Yes
T4	Unclear[b]	Yes	Yes	Yes	Yes	Yes	Yes	Yes	Yes	Yes
T5	Unclear[b]	Yes	Yes	Yes	Yes	Yes	Yes	Yes	Yes	Yes
T6	Yes	Yes	Yes	Yes	Unclear[d]	No	No	Yes	Unclear[d]	Yes
T7	Yes	Yes	Yes	Yes	Yes	No	No	Yes	No	Yes
T8	N/A	Yes	Yes	Yes	Yes	No	Yes	Yes	Yes	Yes
T9	No	Yes	Yes	Yes	Yes	Yes	No	No	N/A[e]	N/A[e]
T10	No	Unclear[f]	Unclear[g]	Unclear[g]	No	No	No	No	No	Unclear[g]
T11	N/A	Unclear[f]	Yes	Yes	Unclear[f]	Unclear[f]	Unclear[f]	Yes	Unclear[f]	Yes
T12	Yes	Yes	Yes	Yes	Yes	Yes	Yes	Yes	Yes	Yes
T13	N/A	No	Yes	Unclear[f]	Unclear[f]	Yes	Yes	Yes	Yes	Yes
T14	Yes	No	Yes	Yes	No	Unclear[h]	Unclear[h]	Yes	Yes	Yes
T15	Yes	No	Yes	Yes	No	Unclear[h]	Unclear[h]	Unclear[h]	No	No

[a] Loss of aromaticity is overemphasized; [b] The aromaticity remains almost unchanged with the distortion;[c] The trend in aromaticity remains almost unchanged with some oscillations; [d] The aromaticity is higher than that of benzene only for a small number of molecules; [e] π orbitals cannot be clearly identified; [f] Fails only in ordering one molecule; [g] Fails only in ordering one molecule. At the CCSD level, this index passed the test; [h] The aromaticity of the TS is higher than that of benzene

As shown in Table 2, NICS(0)$_{\pi zz}$ reproduces perfectly the expected trends for almost all tests of aromaticity and fails only in T10 and T15. In T10, the expected order of aromaticity is benzene > pyridine > pyridazine > pyrimidine > pyrazine > triazine and, as MCI, NICS(0)$_{\pi zz}$ fails only in ordering one molecule of the series and, interestingly, improves the performance of NICS(1)$_{zz}$. T15 corresponds to the thermally allowed [2+2+2] trimerization of acetylene where three acetylenic π-bonds are converted into C–C σ-bonds to form benzene. Previous studies have reported that the system evolves from localized σ and π electrons in the reactants to the well-known π-delocalization in benzene through a TS which has mainly in-plane σ electron delocalization with only minor π electron delocalization [106–108]. Thus, it seems reasonable to think that, in this reaction, the aromatic character of the

6-MR being formed increases more or less uniformly from the initial reactants to the TS. At this point it reduces somewhat along the reaction coordinate until the final increase before reaching the benzene molecule that should be the most aromatic species in the whole reaction coordinate. PDI, MCI, I_{ring}, NICS(0), NICS(1), and NICS(1)$_{zz}$ reproduce the expected trend while NICS(0)$_{\pi zz}$, as FLU and HOMA, fails to detect the maximum of aromaticity in the TS region. Moreover, NICS(0), NICS(1), and NICS(1)$_{zz}$ results find that the transition structure of this reaction is more aromatic than benzene [109–110] and for this reason we consider that the performance of NICS is "unclear" in this test (see Table 2). In order to explain the behavior of NICS(0)$_{\pi zz}$ in T15, we have calculated the values of NICS(0)$_{\sigma zz}$, NICS(0)$_{\pi zz}$, and NICS(0)$_{zz}$ along the reaction path. As can be seen from Figure 5, NICS(0)$_{\sigma zz}$ shows a large diamagnetic character in the TS region whereas NICS(0)$_{\pi zz}$ is almost zero. On the other hand, the trends are reversed when the reaction evolves to the formation of benzene, that is, NICS(0)$_{\pi zz}$ increases while NICS(0)$_{\sigma zz}$ decreases. Interestingly, NICS(0)$_{zz}$ values, that take into account both σ and π components, reflect the expected evolution of aromaticity from reactants to product. Finally, it is worth mentioning that NICS(0)$_{\pi zz}$ cannot be evaluated in all tests, as in T9, because π orbitals cannot be clearly identified. In some cases, as in out-of-plane benzene distortions, although the σ and π orbitals cannot be exactly separated the value of NICS(0)$_{\pi zz}$ can be estimated from the CMO-NICS values of the orbitals that have a larger contribution coming from the out-of-plane p_z orbitals.

Figure 5. Plot of NICS(0)$_{\sigma zz}$ (ppm), NICS(0)$_{\pi zz}$ (ppm), and NICS(0)$_{zz}$ (ppm) *versus* the reaction coordinate (IRP in amu$^{1/2}$·bohr).

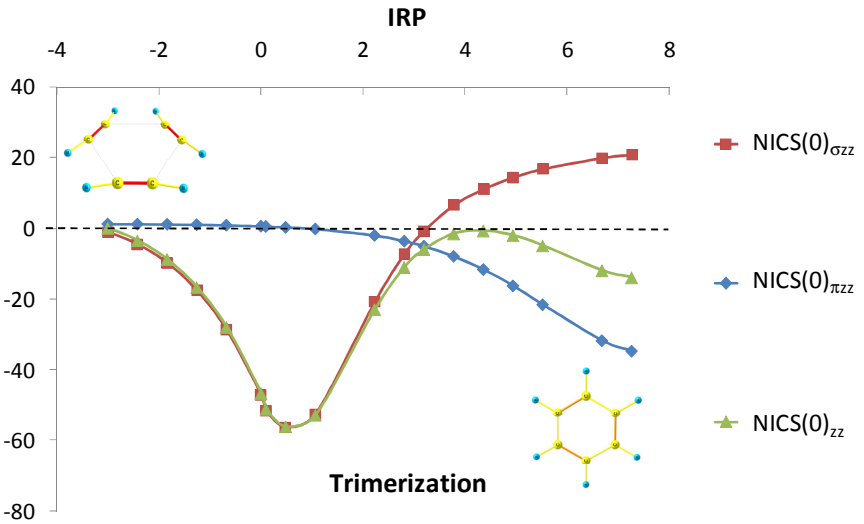

Despite some weaknesses, NICS performs very well to classify inorganic clusters in groups of aromatic, non-aromatic or antiaromatic species. This good performance of NICS is discussed in the next Section.

4. NICS Profiles as Aromaticity Criteria in Inorganic Clusters

Recently, there has been a renewed interest [111–113] in the analysis of NICS values along the perpendicular direction of the molecular ring, the so-called NICS profiles or NICS-scan. Such a

possibility was first discussed by Schleyer [65] in the case of organic compounds, and lately used extensively by Stanger [111,112,114]. Some of us [113] have also analyzed the possibility of using NICS profiles in the analysis of inorganic species. The aromaticity of these compounds is more intricate than the π-aromaticity of their organic counterparts. Therefore, it seems natural to analyze NICS values along the perpendicular direction of the ring, rather than taking single point NICS values as a measure of aromaticity.

Figure 6. Schematic plots representing the three different behaviors of the NICS values from the ring critical point (RCP) up to five angstroms above the ring following an axis perpendicular to the ring plane. The three different kinds of behavior observed are labeled I, II(a,b) and III. Reprinted from Reference [113]. Copyright 2006 Elsevier.

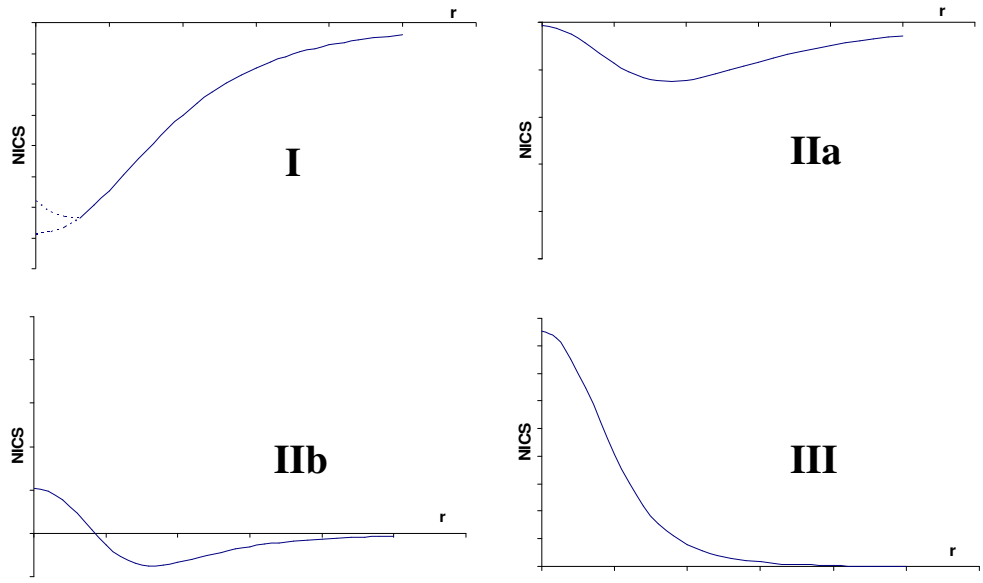

A large set of monocyclic planar inorganic compounds, having aromatic, non-aromatic or antiaromatic character, was chosen as a test set. It was found, not unexpectedly, that all NICS minima neither fall near the ring center nor close to 1 Å above the ring plane. It suggests that both NICS(0) and NICS(1) should be used with caution in inorganic species. Notwithstanding, NICS proved to be useful to qualitatively analyze the aromaticity in inorganic compounds. According to the shape of the NICS profile the molecules were classified into three groups: aromatic, non-aromatic, and anti-aromatic species (see Figure 6). This classification is only qualitative and by no means allows a clear cut distinction between the different groups, and for instance, the non-aromatic group could be further subdivided into species with a rather aromatic character from those with a subtle antiaromatic behavior. However, there have been very few attempts to classify inorganic compounds, mostly based on electron counts or the examination of frontier orbitals, and NICS profiles were among the first tools to provide a clear classification of inorganic species according to their aromaticity.

NICS profiles have also been used to study the change of aromaticity experienced by trigonal alkaline earth metal clusters coordinated to alkaline atoms [52] as well as the effect of $Cr(CO)_6$ coordination in benzene [97]. In addition, Tsipis has recently analyzed $NICS_{zz}$ profiles in several organic and inorganic compounds cages [115] as well as in lanthanide three-membered rings [116].

5. NICS *vs.* MCI Inconsistencies in Inorganic Clusters

In a recent work [52], we found that NICS and the MCI values predicted opposite trends of aromaticity in Mg_3^{2-} when coordinated to alkalimetal cations. Table 3 collects the NICS and MCI values corresponding to free Mg_3^{2-} and Na^+ coordinated to Mg_3^{2-}. All NICS indices show a significant increase in the aromaticity of the ring from Mg_3^{2-} to Na_2Mg_3, while MCI predicts a decrease of aromaticity along the same direction. Similar results were reported by Chattaraj *et al.* for the metal complexation of Al_4^{2-} [51]. Moreover, we also showed [113] that single-point NICS calculations fail to provide correct trends for some particular inorganic clusters. For example, we found unexpectedly that C_{2v} $GeAl_3^-$ is more aromatic than D_{4h} Al_4^{2-} according to NICS(0) values [113].

Table 3. Total and π MCI (in electrons) and NICS (in ppm) indices for Mg_3^{2-} (D_{3h}, $^1A_1$'), $NaMg_3^-$ (C_{3v}, $^1A_1$) and Na_2Mg_3 (D_{3h}, $^1A_1$') calculated at B3LYP/6-311+G(d) level of theory [a].

Index	**Mg_3^{2-}**	**$NaMg_3^-$**	**Na_2Mg_3**
MCI	0.458	0.306	0.255
MCI_π	0.000	0.070	0.066
NICS(0)	-2.85	-22.58	-28.86
$NICS(0)_{ZZ}$	-12.72	-17.92	-21.38
NICS(1)	-4.00	-20.69[b] (-15.33)[c]	-24.07
$NICS(1)_{ZZ}$	-12.21	-21.46[b] (-17.90)[c]	-24.82

[a] From Reference [52]; [b] Measured in the direction to the cation; [c] Measured in the opposite direction to the cation.

As said in the Introduction, the most widely used indicator of aromaticity in inorganic systems is NICS. We have seen, however, that NICS fails to account for the changes of aromaticity in some particular organic molecules. For inorganic clusters, we have shown that in some cases the trends provided by NICS and MCI are divergent. Furthermore, the fact that the π-component of the MCI in Al_4^{2-} is almost the same as that of $C_4H_4^{2+}$ seems to indicate an apparent good behavior of MCI for all-metal clusters [50]. Moreover, we showed that electronic indices such as multicenter indices are superior to NICS to quantify aromaticity in classical organic aromatic systems [73,117]. Therefore, it is reasonable to question the reliability of NICS as a measure of aromaticity in all-metal and semimetal clusters. To analyze the NICS and MCI performances, in a recent work [118], we have studied the 4-MR series of valence isoelectronic inorganic species $[X_nY_{4-n}]^{q\pm}$ (X = Al and Ga, Y = Si and Ge; n = 0 to 4) that have a predictable trend of aromaticity. Thus, one can predict a sudden decrease in aromaticity when going from Al_4^{2-} to, for instance, $SiAl_3^-$ due to the reduction of symmetry and the substitution of one Al atom by a more electronegative Si atom. A smooth reduction of aromaticity when going from Al_3Si^- to Al_2Si_2 is also likely, although more arguable. And the same should occur from Si_4^{2+} to Al_2Si_2. Therefore, for instance, the expected order of aromaticity in the series $[Al_nSi_{4-n}]^{n-2}$ (n = 0 to 4) is $Al_4^{2-} > Al_3Si^- \geq Al_2Si_2 \leq AlSi_3^+ < Si_4^{2+}$. A similar behavior is likely to be present in series where X and Y come from different groups of the Periodic Table. In addition, we have studied two $[P_nY_{5-n}]^{4-n}$

(Y = S and Se; n = 0 to 5) series of 5-MRs. For the series analyzed, it was found that the elements of the $[X_nY_{4-n}]^{q\pm}$ series present σ- and π-aromaticity, while $[P_nY_{5-n}]^{4-n}$ compounds are only π-aromatic.

6. NICS and MCI Assessment in a Series of Inorganic Clusters with Predictable Aromatic Trends

In this section, we briefly summarize the results obtained for the series $[X_nY_{4-n}]^{2-n}$ (n = 0 to 4) where X = Al, Ga and Y = Si, Ge. The number of valence electrons is 14 for all members of these series. The molecular structure of the ground state of X_4^{2-} and Y_4^{2+} clusters is D_{4h} square planar [119]. For X_2Y_2 there are two possible planar structures corresponding to the *cis*- and *trans*-configuration [22,120]. According to previous studies [22,119,121], the *cis*-configuration is more stable for Al_2Si_2, Ga_2Si_2, and Ga_2Ge_2 clusters while the *trans*- is the most stable for Al_2Ge_2. Moreover, Jusélius *et al.* found that the aromaticity of the *cis*- and *trans*-configurations is similar in Al_2Si_2 [121]. In order to make comparisons between series easier, the *cis*-configuration was taken in all the cases.

First, the performance of electronic multicenter indices is evaluated. The MCI and MCI_π obtained for Al_4^{2-} are 0.356 and 0.187 e, respectively. The value of the MCI_π of 0.187 e can be easily and analytically obtained for monodeterminantal wave functions in any ring X_4 of D_{4h} symmetry with only 2π-electrons occupying the same orbital such as in Al_4^{2-}. This result points out that the π delocalization in the Al_4^{2-} species is slightly larger than the σ one (0.187 *vs.* 0.169 e). This is in line with previous dissected NICS results [61] showing that $NICS(0)_\pi$ is somewhat more negative than $NICS(0)_\sigma$ and it is also in agreement with the result from the electronic localization function indicating a higher π- than σ-aromaticity in Al_4^{2-} [122], but in contrast with the fact that the ring current in Al_4^{2-} has a minor contribution from the π-system [123,124]. For symmetry reasons, the MCI_π values of the D_{4h} Ga_4^{2-}, Si_4^{2+}, and Ge_4^{2+} cluster with 2π-electrons is exactly the same as that of Al_4^{2-}, 0.187 e. In all the cases, the MCI and MCI_π values show an abrupt decrease of aromaticity when going from X_4^{2-} to X_3Y^- and from Y_4^{2+} to XY_3^+. Moreover, these indices predict a similar aromaticity for X_3Y^-, X_2Y_2, and XY_3^+ clusters. Interestingly, both total MCI and MCI_π curves have a clear concave ∪ shape providing the expected order of aromaticity in the series analyzed, *i.e.*, $X_4^{2-} > X_3Y^- \geq X_2Y_2 \leq XY_3^+ < Y_4^{2+}$ (see Figure 7 for an example). The only exception is found in the total MCI that yields $AlSi_3^+$ slightly less aromatic than Al_2Si_2.

Next, we analyze whether the NICS indices follow the expected trends of aromaticity for the series analyzed. First, we find that NICS values in inorganic aromatic clusters strongly depend on the point where they are calculated. The NICS value can be calculated at the ring center (NICS(0)) determined by the non-weighted mean of the heavy atoms coordinates and also in the ring critical point (RCP), the point of lowest density in the ring plane, to yield $NICS(0)^{rcp}$ values. Interestingly, while $NICS(0)^{rcp}$ provides the expected trend, NICS(0) fails to predict a steady increase when going from Al_4^{2-} to, for instance, Ge_4^{2+}. Therefore, the NICS values have been calculated at the RCP for all the series analyzed. In general, the NICS measures used in this study reproduce the expected trend, $X_4^{2-} > X_3Y^- \geq X_2Y_2 \leq XY_3^+ < Y_4^{2+}$ (see Figure 7 for an example). $NICS(0)_\pi^{rcp}$, $NICS(0)_{\pi zz}^{rcp}$, and $NICS(1)_{zz}^{rcp}$ performs the best among the different NICS indices analyzed while $NICS(0)^{rcp}$, $NICS(1)^{rcp}$, and $NICS(0)_{zz}^{rcp}$ present some failures. In particular, $NICS(0)^{rcp}$ fails yielding $AlSi_3^+$ slightly more aromatic than Al_2Si_2. When the σ-π separation is applied to MCI and $NICS(0)^{rcp}$ indices, MCI_π, $NICS(0)_\pi^{rcp}$, and $NICS(0)_{\pi zz}^{rcp}$ show the expected ∪ shape while MCI_σ and $NICS(0)_\sigma$ constantly

decrease when going from X_4^{2-} to XY_3^+. Then the σ-aromaticity abruptly increases from XY_3^+ to full symmetric Y_4^{2+}. In general, MCI_σ and $NICS(0)_\sigma$ tend to decrease when group 13 atoms (Al, Ga) are substituted by group 14 atoms (Si, Ge), except when the D_{4h} structure is reached. This fact leads to a slightly lower σ-aromaticity in XY_3^+ than X_2Y_2. However, this effect is in most cases cancelled out by the π-contribution when total MCI and NICS indices are analyzed and, consequently, the expected ∪ shape is observed.

Figure 7. Variation of MCI, MCI_π, and MCI_σ (in electrons), and NICS (ppm) indices calculated at the ring critical point (RCP) along the series Al_4^{2-}, Al_3Ge^-, Al_2Ge_2, $AlGe_3^+$, and Ge_4^{2+}. Reprinted from Reference [96]. Copyright 2010 American Chemical Society.

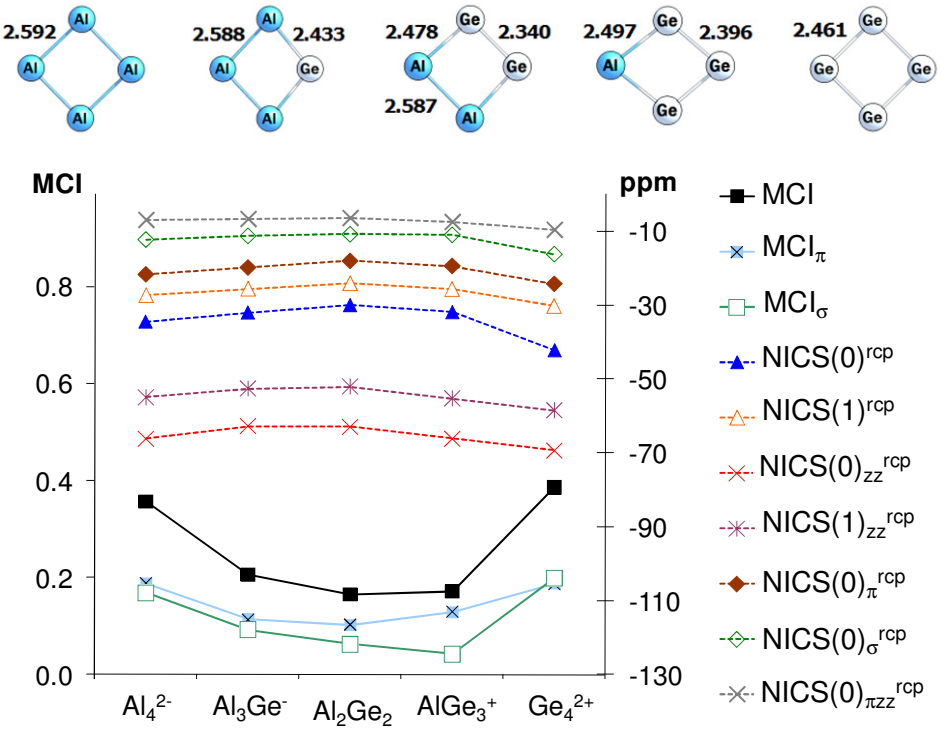

Finally, we discuss the $[P_nY_{5-n}]^{n-4}$ (Y = S and Se; n = 0 to 5) series of 5-MR clusters. Among these series, P_5^- is the only inorganic cluster that has been studied previously both experimentally and with theoretical methodologies [21,125–128]. These works show by means of photoelectron spectroscopy and *ab initio* calculations that D_{5h} P_5^- is a global minimum and possesses six π-electrons in three π molecular orbitals, resulting in π-aromaticity according to the Hückel's 4n + 2 rule. Figure 8 depicts the molecular structure, MCI, and NICS values for the valence isoelectronic $[P_nSe_{5-n}]^{n-4}$ (n = 0 to 5) clusters. In line with the previously observed π-aromaticity of P_5^-, the MCI and MCI_π values of P_5^- differ by only 0.001 e indicating that the contribution of the σ-electrons to the total MCI value is irrelevant. The same is true for all the members of these two series. As to the trends depicted in Figure 8, it is found that MCI and MCI_π curves present the expected ∪ shape (only MCI is represented in Figure 8 since MCI and MCI_π plots are almost identical). However, all NICS values yield a continuous reduction of aromaticity along the series P_5^- to Se_5^{4+}. Dissected NICS calculations help to understand this trend. Remarkably, $NICS(0)_\pi^{rcp}$ and $NICS(0)_{\pi zz}^{rcp}$ differ from the rest of NICS indices, showing a similar behavior to MCI and MCI_π. $NICS(0)_\pi^{rcp}$ values yield Se_5^{4+} more aromatic than P_5^-

while $NICS(0)_{\pi zz}^{rcp}$ shows the opposite trend. The first only fails assigning a more aromatic character to $P_3Se_2^+$ than to P_4Se and the latter overestimates the aromaticity of $P_2Se_3^{2+}$ in comparison with PSe_4^{3+}. Analogous results are obtained for the $[P_nS_{5-n}]^{n-4}$ series.

Figure 8. Molecular structure (in Å) and variation of MCI (in electrons), and NICS (ppm) indices calculated at the ring critical point (RCP) along the series P_5^-, P_4Se, $P_3Se_2^+$, $P_2Se_3^{2+}$, PSe_4^{3+}, and Se_5^{4+}. Reprinted from Reference [96]. Copyright 2010 American Chemical Society.

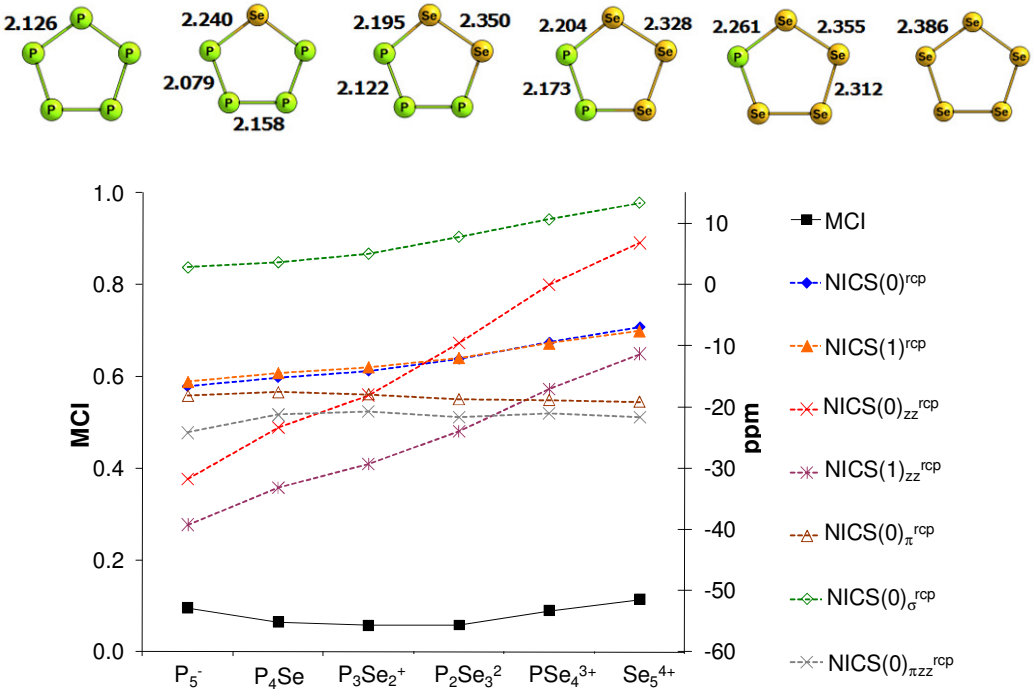

7. Conclusions

Our results indicate that the multicenter indices perform generally better than NICS, especially the MCI_π, for measuring the local aromaticity of classical organic molecules and all-metal and semimetal aromatic clusters. As to NICS, we found a superior behavior of $NICS(0)_{\pi zz}$ as compared to NICS(0), NICS(1), and their corresponding out-of-plane components. Indeed, $NICS(0)_{\pi zz}$ give the correct trends for the studied all-metal and semimetal clusters, except for the relative aromaticity of two compounds in the $[P_nSe_{5-n}]^{n-4}$ series. In addition, $NICS(0)_{\pi zz}$ fails only in two tests on classical aromatic organic species: T9 and T15.

NICS and MCI are indices of aromaticity that do not require reference values and, consequently, they are likely the most useful indicators of aromaticity for inorganic clusters. The present study reveals that if one wants to order a series of inorganic compounds according to their aromaticity, it is recommendable to use multicenter electronic indices or $NICS(0)_\pi$ and $NICS(0)_{\pi zz}$ values. For this purpose, neither NICS(0) nor NICS(1) are reliable enough. However, all-metal and semimetal clusters present multi-fold aromaticity and, in some cases, the analysis of the π component is not enough to describe the aromaticity of the system. Consequently, it is also recommended to analyze the σ-, π-, and δ-counterparts of the multicenter electronic indices and dissected NICS values. On the other hand, if

one only wants to discuss whether a given cluster is aromatic or not, then both MCI and NICS, and particularly NICS-scan, do a good job to classify all-metal and semimetal clusters into aromatic, nonaromatic, and antiaromatic.

Acknowledgements

Financial help has been furnished by the Spanish MICINN Project No. CTQ2008-03077/BQU and by the Catalan DIUE through project No. 2009SGR637. F.F. and J.P. thank the MICINN for the doctoral fellowship No. AP2005-2997 and the Ramón y Cajal contract, respectively. E.M. acknowledges financial support from the Lundbeck Foundation Center and from Marie Curie IntraEuropean Fellowship, Seventh Framework Programme (FP7/2007-2013), under grant agreement No. PIEF-GA-2008-221734 and from the Polish Ministry of Science and Higher Education (Project No. N N204 215634). Support for the research of M.S. was received through the prize "ICREA Academia" 2009 for excellence in research funded by the DIUE of the Generalitat de Catalunya. We thank the Centre de Supercomputació de Catalunya (CESCA) for partial funding of computer time.

References and Notes

1. Schleyer, P.v.R. Introduction: Aromaticity. *Chem. Rev.* **2001**, *101*, 1115–1118.
2. Schleyer, P.v.R. Introduction: Delocalization–Pi and Sigma. *Chem. Rev.* **2005**, *105*, 3433–3435.
3. Heilbronner, E. Hückel Molecular Orbitals of Möbius-Type Conformation of Annulenes *Tetrahedron Lett.* **1964**, *5*, 1923–1928.
4. Rzepa, H.S. Möbius Aromaticity and Delocalization. *Chem. Rev* **2005**, *105*, 3697–3715.
5. Bühl, M.; Hirsch, A. Spherical Aromaticity of Fullerenes. *Chem. Rev.* **2001**, *101*, 1153–1183.
6. Chen, Z.F.; King, R. Spherical Aromaticity: Recent Work on Fullerenes, Polyhedral Boranes, and Related Structures. *Chem. Rev.* **2005**, *105*, 3613–3642.
7. Masui, H. Metalloaromaticity. *Coord. Chem. Rev.* **2001**, *219*, 957–992.
8. Dewar, M.J.S.; McKee, M.L. Aspects of Cyclic Conjugation. *Pure Appl. Chem.* **1980**, *52*, 1431–1441.
9. Dewar, M.J.S. Chemical Implications of Sigma Conjugation. *J. Am. Chem. Soc.* **1984**, *106*, 669–682.
10. Cremer, D.; Gauss, J. Theoretical Determination of Molecular Structure and Conformation. 20. Reevaluation of the Strain Energies of Cyclopropane and Cyclobutane-CC and CH Bond Energies, 1, 3 Interactions, and σ-Aromaticity. *J. Am. Chem. Soc.* **1986**, *108*, 7467–7477.
11. Li, X.; Kuznetsov, A.E.; Zhang, H.-F.; Boldyrev, A.; Wang, L.-S. Observation of All-Metal Aromatic Molecules. *Science* **2001**, *291*, 859–861.
12. Boldyrev, A.I.; Wang, L.-S. All-Metal Aromaticity and Antiaromaticity. *Chem. Rev.* **2005**, *105*, 3716–3757.
13. Tsipis, C.A. DFT Study of "All-Metal" Aromatic Compounds. *Coord. Chem. Rev.* **2005**, *249*, 2740–2762.
14. Zubarev, D.Y.; Averkiev, B.B.; Zhai, H.-J.; Wang, L.-S.; Boldyrev, A.I. Aromaticity and Antiaromaticity in Transition-Metal Systems. *Phys. Chem. Chem. Phys.* **2008**, *10*, 257–267.

15. Huang, X.; Zhai, H.-J.; Kiran, B.; Wang, L.-S. Observation of *d*-Orbital Aromaticity. *Angew. Chem. Int. Ed.* **2005**, *44*, 7251–7254.
16. Zhai, H.-J.; Averkiev, B.B.; Zubarev, D.Y.; Wang, L.-S.; Boldyrev, A.I. *δ* Aromaticity in $[Ta_3O_3]^-$. *Angew. Chem. Int. Ed.* **2007**, *46*, 4277-4280.
17. Averkiev, B.B.; Boldyrev, A.I. Hf_3 Cluster Is Triply (*σ*-, π-, and δ-) Aromatic in the Lowest D_{3h}, $^1A_1$ State. *J. Phys. Chem. A* **2007**, *111*, 12864–12866.
18. Tsipis, A.C.; Kefalidis, C.E.; Tsipis, C.A. The Role of the 5*f* Orbitals in Bonding, Aromaticity, and Reactivity of Planar Isocyclic and Heterocyclic Uranium Clusters. *J. Am. Chem. Soc.* **2008**, *130*, 9144–9155.
19. Zhan, C.-G.; Zheng, F.; Dixon, D.A. Electron Affinities of Al_n Clusters and Multiple-Fold Aromaticity of the Square Al_4^{2-} Structure. *J. Am. Chem. Soc.* **2002**, *124*, 14795–14803.
20. Zhai, H.-J.; Kuznetsov, A.E.; Boldyrev, A.; Wang, L.-S. Multiple Aromaticity and Antiaromaticity in Silicon Clusters. *Chem. Phys. Chem.* **2004**, *5*, 1885–1891.
21. Liu, Z.-Z.; Tian, W.-Q.; Feng, J.-K.; Zhang, G.; Li, W.-Q. Theoretical Study on Structures and Aromaticities of P_5^- Anion, $[Ti(\eta^5\text{-}P_5)]^-$ and Sandwich Complex $[Ti(\eta^5\text{-}P_5)_2]^{2-}$. *J. Phys. Chem. A* **2005**, *109*, 5645–5655.
22. Chi, X.X.; Chen, X.J.; Yuan, Z.S. Theoretical Study in the Aromaticity of the Bimetallic Clusters X_2M_2 (X = Si, Ge; M = Al, Ga). *J. Mol. Struct. (Theochem)* **2005**, *732*, 149–153.
23. Krygowski, T.M.; Cyrański, M.K. Structural Aspects of Aromaticity. *Chem. Rev.* **2001**, *101*, 1385–1419.
24. Krygowski, T.M.; Cyrański, M.K.; Czarnocki, Z.; Häfelinger, G.; Katritzky, A.R. Aromaticity: A Theoretical Concept of Immense Practical Importance. *Tetrahedron* **2000**, *56*, 1783–1796.
25. Chen, Z.; Wannere, C.S.; Corminboeuf, C.; Puchta, R.; Schleyer, P.v.R. Nucleus-Independent Chemical Shifts (NICS) as an Aromaticity Criterion. *Chem. Rev.* **2005**, *105*, 3842–3888.
26. Cyrański, M.K. Energetic Aspects of Cyclic pi-electron Delocalization: Evaluation of the Methods of Estimating Aromatic Stabilization Energies. *Chem. Rev.* **2005**, *105*, 3773–3811.
27. Poater, J.; Duran, M.; Solà, M.; Silvi, B. Theoretical Evaluation of Electron Delocalization in Aromatic Molecules by Means of Atoms in Molecules (AIM) and Electron Localization Function (ELF) Topological Approaches. *Chem. Rev.* **2005**, *105*, 3911–3947.
28. Merino, G.; Vela, A.; Heine, T. Description of Electron Delocalization via the Analysis of Molecular Fields. *Chem. Rev.* **2005**, *105*, 3812–3841.
29. Poater, J.; García-Cruz, I.; Illas, F.; Solà, M. Discrepancy Between Common Local Aromaticity Measures in a Series of Carbazole Derivatives. *Phys. Chem. Chem. Phys.* **2004**, *6*, 314–318.
30. Katritzky, A.R.; Barczynski, P.; Musumarra, G.; Pisano, D.; Szafran, M. Aromaticity as a Quantitative Concept. 1. A Statistical Demostration of the Orthogonality of "Classical" and "Magnetic" Aromaticity in Five- and Six- Membered Heterocycles. *J. Am. Chem. Soc.* **1989**, *111*, 7–15.
31. Katritzky, A.R.; Karelson, M.; Sild, S.; Krygowski, T.M.; Jug, K. Aromaticity as a Quantitative Concept. 7. Aromaticity Reaffirmed as a Multidimensional Characteristic. *J. Org. Chem.* **1998**, *63*, 5228–5231.
32. Cyrański, M.K.; Krygowski, T.M.; Katritzky, A.R.; Schleyer, P.v.R. To What Extent Can Aromaticity Be Defined Uniquely? *J. Org. Chem.* **2002**, *67*, 1333–1338.

33. Jug, K.; Köster, A.M. Aromaticity as a Multi-Dimensional Phenomenon. *J. Phys. Org. Chem.* **1991**, *4*, 163–169.
34. Kruszewski, J.; Krygowski, T.M. Definition of Aromaticity Basing on the Harmonic Oscillator Model. *Tetrahedron Lett.* **1972**, *13*, 3839–3842.
35. Krygowski, T.M. Crystallographic studies of Inter- and Intra-Molecular Interactions Reflected in benzenoid Hydrocarbons. Nonequivalence of Indices of Aromaticity. *J. Chem. Inform. Comput. Sci.* **1993**, *33*, 70–78.
36. Matito, E.; Duran, M.; Solà, M. The Aromatic Fluctuation Index (FLU): A New Aromaticity Index Based on Electron Delocalization. *J. Chem. Phys.* **2005**, *122*, 014109.
37. Bultinck, P.; Ponec, R.; Van Damme, S. Multicenter Bond Indices as a New Measure of Aromaticity in Polycyclic Aromatic Hydrocarbons. *J. Phys. Org. Chem.* **2005**, *18*, 706–718.
38. Matta, C.F. Application of the Quantum Theory of Atoms in Molecules to Selected Physico-Chemical and Biophysical Problems: Focus on Correlation with Experiment. *J. Comput. Chem.* **2003**, *24*, 453–462.
39. Matta, C.F.; Hernández-Trujillo, J. Bonding in Polycyclic Aromatic Hydrocarbons in Terms of the Electron Density and of Electron Delocalization. *J. Phys. Chem. A* **2003**, *107*, 7496–7504.
40. Boldyrev, A.I.; Kuznetsov, A.E. On the Resonance Energy in New All-Metal Aromatic Molecules. *Inorg. Chem.* **2002**, *41*, 532–537.
41. Hückel, E. Quantentheoretische Beiträge zum Benzolproblem I. Die Elektronenkonfiguration des Benzols und Verwandter Verbindungen. *Z. Physik* **1931**, *70*, 104–186.
42. Hückel, E. Quanstentheoretische Beiträge zum Benzolproblem II. Quantentheorie der Induzierten Polaritäten. *Z. Physik* **1931**, *72*, 310–337.
43. Hückel, E. Quantentheoretische Beiträge zum Problem der Aromatischen und Ungesättigten Verbindungen. III. *Z. Physik* **1932**, *76*, 628–648.
44. Hückel, E. The Theory of Unsaturated and Aromatic Compounds. *Z. Elektrochemie* **1937**, *43*, 752–788, 827–849.
45. Schleyer, P.v.R.; Maerker, C.; Dransfeld, A.; Jiao, H.; van Eikema Hommes, N.J.R. Nucleus-Independent Chemical Shifts: A simple and Efficient Aromaticity Probe. *J. Am. Chem. Soc.* **1996**, *118*, 6317–6318.
46. Giambiagi, M.; de Giambiagi, M.S.; dos Santos, C.D.; de Figueiredo, A.P. Multicenter Bond Indices as a Measure of Aromaticity. *Phys. Chem. Chem. Phys.* **2000**, *2*, 3381–3392.
47. Bultinck, P.; Rafat, M.; Ponec, R.; van Gheluwe, B.; Carbó-Dorca, R.; Popelier, P. Electron Delocalization and Aromaticity in Linear Polyacenes: Atoms in Molecules Multicenter Delocalization Index. *J. Phys. Chem. A* **2006**, *110*, 7642–7648.
48. Mandado, M.; González-Moa, M.J.; Mosquera, R.A. QTAIM N-Center Delocalization Indices as Descriptors of Aromaticity in Mono and Poly Heterocycles. *J. Comput. Chem.* **2007**, *28*, 127–136.
49. Cioslowski, J.; Matito, E.; Solà, M. Properties of Aromaticity Indices Based on the One-Electron Density Matrix. *J. Phys. Chem. A* **2007**, *111*, 6521–6525.
50. Mandado, M.; Krishtal, A.; Van Alsenoy, C.; Bultinck, P.; Hermida-Ramón, J.M. Bonding Study in All-Metal Clusters Containing Al_4 Units. *J. Phys. Chem. A* **2007**, *111*, 11885–11893.

51. Roy, D.R.; Bultinck, P.; Subramanian, V.; Chattaraj, P.K. Bonding, Reactivity and Aromaticity in the Light of the Multicenter Indices. *J. Mol. Struct. (Theochem)* **2008**, *854*, 35–39.
52. Jiménez-Halla, J.O.C.; Matito, E.; Blancafort, L.; Robles, J.; Solà, M. Tuning Aromaticity in Trigonal Alkaline Earth Metal Clusters and Their Alkali Metal Salts. *J. Comput. Chem.* **2009**, *30*, 2764–2776.
53. Havenith, R.W.A.; Fowler, P.W.; Steiner, E.; Shetty, S.; Kanhere, D.; Pal, S. Aromaticity and Antiaromaticity of Li_xAl_4 Clusters: Ring Current Patterns *Versus* Electron Counting. *Phys. Chem. Chem. Phys.* **2004**, *6*, 285–288.
54. Jung, Y.; Heine, T.; Schleyer, P.v.R.; Head-Gordon, M. Aromaticity of Four-Membered-Ring 6π-electron Systems: N_2S_2 and $Li_2C_4H_4$. *J. Am. Chem. Soc.* **2004**, *126*, 3132–3138.
55. Aihara, J.; Kanno, H.; Ishida, T. Aromaticity of Planar Boron Clusters Confirmed. *J. Am. Chem. Soc.* **2005**, *127*, 13324–13330.
56. Tsipis, A.C.; Tsipis, C.A. Hydrometal Analogues of Aromatic Hydrocarbons: A New Class of Cyclic Hydrocoppers (I). *J. Am. Chem. Soc.* **2003**, *125*, 1136–1137.
57. Tsipis, C.A.; Karagiannis, E.E.; Kladou, P.F.; Tsipis, A.C. Aromatic Gold and Silver Rings: Hydrosilver (I) and Hydrogold (I) Analogues of Aromatic Hydrocarbons. *J. Am. Chem. Soc.* **2004**, *126*, 12916–12929.
58. Wannere, C.S.; Corminboeuf, C.; Wang, Z.-X.; Wodrich, M.D.; King, R.B.; Schleyer, P.v.R. Evidence for d Orbital Aromaticity in Square Planar Coinage Metal Clusters. *J. Am. Chem. Soc.* **2005**, *127*, 5701–5705.
59. Corminboeuf, C.; Wannere, C.S.; Roy, D.; King, R.B.; Schleyer, P.v.R. Octahedral and Tetrahedral Coinage Metal Clusters: Is Three-Dimensional d-Orbital Aromaticity Viable? *Inorg. Chem.* **2006**, *45*, 214–219.
60. Zhang, G.H.; Zhao, Y.F.; Wu, J.I.; Schleyer, P.v.R. Ab Initio Study of the Geometry, Stability, and Aromaticity of the Cyclic $S_2N_3^+$ Cation Isomers and Their Isoelectronic Analogues. *Inorg. Chem.* **2009**, *48*, 6773–6780.
61. Chen, Z.; Corminboeuf, C.; Heine, T.; Bohmann, J.; Schleyer, P.v.R. Do All-Metal Antiaromatic Clusters Exist? *J. Am. Chem. Soc.* **2003**, *125*, 13930–13931.
62. Lazzeretti, P. Ring Currents. In *Progress in Nuclear Magnetic Resonance Spectroscopy*; Emsley, J.W., Feeney, J., Sutcliffe, L.H., Eds.; Elsevier: Amsterdam, The Netherlands, 2000; pp. 1–88.
63. Lazzeretti, P. Assessment of Aromaticity Via Molecular Response Properties. *Phys. Chem. Chem. Phys.* **2004**, *6*, 217–223.
64. Aihara, J. Nucleus-Independent Chemical Shifts and Local Aromaticities in Large Polycyclic Aromatic Hydrocarbons. *Chem. Phys. Lett.* **2002**, *365*, 34–39.
65. Schleyer, P.v.R.; Manoharan, M.; Wang, Z.X.; Kiran, B.; Jiao, H.J.; Puchta, R.; van Eikema Hommes, N.J.R. Dissected Nucleus-Independent Chemical Shift Analysis of π-Aromaticity and Antiaromaticity. *Org. Lett.* **2001**, *3*, 2465–2468.
66. Corminboeuf, C.; Heine, T.; Seifert, G.; Schleyer, P.v.R.; Weber, J. Induced Magnetic Fields in Aromatic [n]-Annulenes–Interpretation of NICS Tensor Components. *Phys. Chem. Chem. Phys.* **2004**, *6*, 273–276.
67. Schleyer, P.v.R.; Manoharan, M.; Jiao, H.J.; Stahl, F. The Acenes: Is There a Relationship Between Aromatic Stabilization and Reactivity? *Org. Lett.* **2001**, *3*, 3643–3646.

68. Schleyer, P.v.R.; Jiao, H.J.; van Eikema Hommes, N.J.R.; Malkin, V.G.; Malkina, O.L. An Evaluation of the Aromaticity of Inorganic Rings: Refined Evidence From Magnetic Properties. *J. Am. Chem. Soc.* **1997**, *119*, 12669–12670.
69. Corminboeuf, C.; Heine, T.; Weber, J. Evaluation of Aromaticity: A New Dissected NICS Model Based On Canonical Orbitals. *Phys. Chem. Chem. Phys.* **2003**, *5*, 246–251.
70. Glendening, E.D.; Badenhoop, J.K.; Reed, A.E.; Carpenter, J.E.; Bohmann, J.A.; Morales, C.M.; Weinhold, F. NBO 5.0 Program. Theoretical Chemistry Institute, University of Wisconsin: Madison, WI, USA, 2001.
71. Reed, A.E.; Curtiss, L.A.; Weinhold, F. Intermolecular Interactions from a Natural Bond Orbital, Donor-Acceptor Viewpoint. *Chem. Rev.* **1988**, *88*, 899–926.
72. Fallah-Bagher-Shaidaei, H.; Wannere, C.S.; Corminboeuf, C.; Puchta, R.; Schleyer, P.v.R. Which NICS Aromaticity Index for Planar Rings Is Best? *Org. Lett.* **2006**, *8*, 863–866.
73. Feixas, F.; Matito, E.; Poater, J.; Solà, M. On the Performance of Some Aromaticity Indices: A Critical Assessment Using a Test Set. *J. Comput. Chem.* **2008**, *29*, 1543–1554.
74. Katritzky, A.R.; Jug, K.; Oniciu, D.C. Quantitative Measures of Aromaticity For mono-, Bi-, and Tricyclic Penta- and Hexaatomic Heteroaromatic Ring Systems and Their Interrelationships. *Chem. Rev.* **2001**, *101*, 1421–1449.
75. Poater, J.; Fradera, X.; Duran, M.; Solà, M. The Delocalization Index as an Electronic Aromaticity Criterion. Application to a Series of Planar Polycyclic Aromatic Hydrocarbons. *Chem. Eur. J.* **2003**, *9*, 400–406.
76. Steiner, E.; Fowler, P.W. Ring Currents in Aromatic Hydrocarbons. *Int. J. Quant. Chem.* **1996**, *60*, 609–616.
77. Steiner, E.; Fowler, P.W.; Havenith, R.W.A. Current Densities of Localized and Delocalized Electrons in Molecules. *J. Phys. Chem. A* **2002**, *106*, 7048–7056.
78. Poater, J.; Solà, M.; Viglione, R.G.; Zanasi, R. The Local Aromaticity of the Six-Membered Rings in Pyracylene. A Difficult Case for the NICS Indicator of Aromaticity. *J. Org. Chem.* **2004**, *69*, 7537–7542.
79. Solà, M.; Mestres, J.; Duran, M. Molecular-Size and Pyramidalization–2 Keys for Understanding the Reactivity of Fullerenes. *J. Phys. Chem.* **1995**, *99*, 10752–10758.
80. Kraakman, P.A.; Valk, J.M.; Niederlander, H.A.G.; Brouwer, D.B.E.; Bickelhaupt, F.M.; Dewolf, W.H.; Bickelhaupt, F.; Stam, C.H. Unusual Reactivity of Small Cyclophanes–Nucleophilic Attack on 11-Chloro[5]Metacyclophane and 8,11-Dichloro[5]Metacyclophane. *J. Am. Chem. Soc.* **1990**, *112*, 6638–6646.
81. Gready, J.E.; Hambley, T.W.; Kakiuchi, K.; Kobiro, K.; Sternhell, S.; Tansey, C.W.; Tobe, Y. NMR-Studies of Bond Order in Distorted Aromatic Systems. *J. Am. Chem. Soc.* **1990**, *112*, 7537–7540.
82. Bodwell, G.J.; Bridson, J.N.; Houghton, T.J.; Kennedy, J.W.J.; Mannion, M.R. 1,8-Dioxa[8](2,7)Pyrenophane, a Severely Distorted Polycyclic Aromatic Hydrocarbon. *Angew. Chem. Int. Ed. Eng.* **1996**, *35*, 1320–1321.
83. Bodwell, G.J.; Bridson, J.N.; Houghton, T.J.; Kennedy, J.W.J.; Mannion, M.R. 1,7-Dioxa[7](2,7)Pyrenophane: The Pyrene Moiety is More Bent Than That of C_{70}. *Chem. Eur. J.* **1999**, *5*, 1823–1827.

84. Bodwell, G.J.; Bridson, J.N.; Cyranski, M.K.; Kennedy, J.W.J.; Krygowski, T.M.; Mannion, M.R.; Miller, D.O. Nonplanar Aromatic Compounds. 8. Synthesis, Crystal Structures, and Aromaticity Investigation of the 1,n-Dioxa[n]Pyrenophanes. How Does Bending Affect the Cyclic π-Electron Delocalization of the Pyrene System? *J. Org. Chem.* **2003**, *68*, 2089–2098.
85. Jenneskens, L.W.; Vaneenige, E.N.; Louwen, J.N. A P-Orbital Axis Vector (POAV) Analysis of Boat-Shaped Benzenes. *New J. Chem.* **1992**, *16*, 775–779.
86. Grimme, S. Theoretical-Study of [4]Paracyclophane and Its Dewar Benzene and Prismane Valence Isomers. *J. Am. Chem. Soc.* **1992**, *114*, 10542–10547.
87. Dijkstra, F.; van Lenthe, J.H. Aromaticity of Bent Benzene Rings: A VBSCF Study. *Int. J. Quant. Chem.* **1999**, *74*, 213–221.
88. Zhigalko, M.V.; Shishkin, O.V.; Gorb, L.; Leszczynski, J. Out-of-plane Deformability of Aromatic Systems in Naphthalene, Anthracene and Phenanthrene. *J. Mol. Struct.* **2004**, *693*, 153–159.
89. Lazzeretti, P.; Malagoni, M.; Zanasi, R. Computational Approach to Molecular Magnetic Properties by Continuous Transformation of the Origin of the Current Density. *Chem. Phys. Lett.* **1994**, *220*, 299–304.
90. Fowler, P.W.; Steiner, E.; Cadioli, B.; Zanasi, R. Distributed-Gauge Calculations of Current Density Maps, Magnetizabilities, and Shieldings for a Series of Neutral and Dianionic Fused Tetracycles: Pyracylene ($C_{14}H_8$), Acepleiadylene ($C_{16}H_{10}$), and Dipleiadiene ($C_{18}H_{12}$). *J. Phys. Chem. A* **1998**, *102*, 7297–7302.
91. Poater, J.; Bofill, J.M.; Alemany, P.; Solà, M. The Role of Electron Density and Magnetic Couplings on the NICS Profiles of [2.2]Paracyclophane and Related Species. *J. Org. Chem.* **2006**, *71*, 1700–1702.
92. Caramori, G.F.; Galembeck, S.E.; Laali, K.K. A Computational Study of [2.2]Cyclophanes. *J. Org. Chem.* **2005**, *70*, 3242–3250.
93. Johnson, C.E.; Bovey, F.A. Calculation of Nuclear Magnetic Resonance Spectra of Aromatic Hydrocarbons. *J. Chem. Phys.* **1958**, *29*, 1012–1014.
94. Portella, G.; Poater, J.; Bofill, J.M.; Alemany, P.; Solà, M. Local Aromaticity of [n]Acenes, [n]Phenacenes, and [n]Helicenes (n = 1–9). *J. Org. Chem.* **2005**, *70*, 2509–2521.
95. Portella, G.; Poater, J.; Bofill, J.M.; Alemany, P.; Solà, M. Erratum of Local Aromaticity of [n]Acenes, [n]Phenacenes, and [n]Helicenes (n = 1–9). *J. Org. Chem.* **2005**, *70*, 4560–4560.
96. Osuna, S.; Poater, J.; Bofill, J.M.; Alemany, P.; Solà, M. Are Nucleus-Independent (NICS) and ^{1}H NMR Chemical Shifts Good Indicators of Aromaticity in π-Stacked Polyfluorenes? *Chem. Phys. Lett.* **2006**, *428*, 191–195.
97. Feixas, F.; Jiménez-Halla, J.O.C.; Matito, E.; Poater, J.; Solà, M. Is the Aromaticity of the Benzene Ring in the (η^6-C_6H_6)$Cr(CO)_3$ Complex Larger Than That of the Isolated Benzene Molecule? *Pol. J. Chem.* **2007**, *81*, 783–797.
98. Mitchell, R.H. Measuring Aromaticity by NMR. *Chem. Rev.* **2001**, *101*, 1301–1315.
99. Mitchell, R.H.; Brkic, Z.; Berg, D.J.; Barclay, T.M. Effective Aromaticity of Tricarbonylchromiumbenzene, about 25 Enhanced over that of Benzene: Structural Evidence from a Complexed Benzannulene. *J. Am. Chem. Soc.* **2002**, *124*, 11983–11988.

100. Mitchell, R.H.; Chen, Y.; Khalifa, N.; Zhou, P. The Synthesis, Aromaticity, and NMR Properties of [14]Annulene Fused Organometallics. Determination of the Effective Bond Localizing Ability ("Relative Aromaticity") and Diamagnetic Anisotropy of Several Organometallic Moieties. *J. Am. Chem. Soc.* **1998**, *120*, 1785–1794.
101. Mitchell, R.H.; Zhou, P.; Venugopalan, S.; Dingle, T.W. Synthesis of the First Metal-Complexed Benzannulene. An Estimate of the Aromaticity of Tricarbonylchromium-Complexed Benzene Relative to the Aromaticity of Benzene Itself. *J. Am. Chem. Soc.* **1990**, *112*, 7812–7813.
102. Low, A.A.; Hall, M.B. Benzene Chromium Tricarbonyl Revisited: Theoretical Study of The Structure and Dynamics of (π^6-C_6H_6)$Cr(CO)_3$. *Int. J. Quant. Chem.* **2000**, *77*, 152–160.
103. Hubig, S.M.; Lindeman, S.V.; Kochi, J.K. Charge Transfer Bonding in Metal-Arene Coordination. *Coord. Chem. Rev.* **2006**, *200-202*, 831–873.
104. Albright, T.A.; Hofmann, P.; Hoffmann, R.; Lillya, C.P.; Dobosh, P.A. Haptotropic Rearrangements of Polyene-ML_n Complexes. 2. Bicyclic Polyene-MCp-$M(CO)_3$ Systems. *J. Am. Chem. Soc.* **1983**, *105*, 3396–3411.
105. Arrais, A.; Diana, E.; Gervasio, G.; Gobetto, R.; Marabello, D.; Stanghellini, P.L. Synthesis, Structural and Spectroscopic Characterization of Four [(η^6-PAH)$Cr(CO)_3$] Complexes (PAH=Pyrene, Perylene, Chrysene, 1,2-Benzanthracene). *Eur. J. Inorg. Chem.* **2004**, 1505–1513.
106. Havenith, R.W.A.; Fowler, P.W.; Jenneskens, L.W.; Steiner, E. Trimerization of Ethyne: Growth and Evolution of Ring Currents in the Formation of the Benzene Ring. *J. Phys. Chem. A* **2003**, *107*, 1867–1871.
107. Santos, J.C.; Polo, V.; Andrés, J. An Electron Localization Function Study of the Trimerization of Acetylene: Reaction Mechanism and Development of Aromaticity. *Chem. Phys. Lett.* **2005**, *406*, 393–397.
108. Mandado, M.; González-Moa, M.J.; Mosquera, R.A. Characterization of Pericyclic Reactions Using Multicenter Electron Delocalization Analysis. *ChemPhysChem* **2007**, *8*, 696–702.
109. Jiao, H.; Schleyer, P.v.R. Aromaticity of Pericyclic Reaction Transition Structures: Magnetic Evidence. *J. Phys. Org. Chem.* **1998**, *11*, 655–662.
110. Morao, I.; Cossio, F.P. A Simple Ring Current Model For Describing in-plane Aromaticity in Pericyclic Reactions. *J. Org. Chem.* **1999**, *64*, 1868-1874.
111. Stanger, A. Nucleus-Independent Chemical Shifts (NICS): Distance Dependence and Revised Criteria for Aromaticity and Antiaromaticity. *J. Org. Chem.* **2006**, *71*, 883–893.
112. Stanger, A. Can Substituted Cyclopentadiene Become Aromatic or Antiaromatic? *Chem. Eur. J.* **2006**, *12*, 2745–2751.
113. Jiménez-Halla, J.O.C.; Matito, E.; Robles, J.; Solà, M. Nucleus-Independent Chemical Shift (NICS) Profiles in a Series of Monocyclic Planar Inorganic Compounds. *J. Organomet. Chem.* **2006**, *691*, 4359–4366.
114. Stanger, A. What Is Aromaticity: A Critique of the Concept of Aromaticity–Can It Really Be Defined? *Chem. Commun.* **2009**, 1939–1947
115. Tsipis, A.C. Efficiency of the $NICS_{zz}$-scan Curves to Probe the Antiaromaticity of Organic and Inorganic Rings/Cages. *Phys. Chem. Chem. Phys.* **2009**, *11*, 8244–8261.

116. Tsipis, A.C.; Depastas, I.G.; Karagiannis, E.E.; Tsipis, C.A. Diagnosis of Magnetoresponsive Aromatic and Antiaromatic Zones in Three-Membered Rings of d- and f-Block Elements. *J. Comput. Chem.* **2010**, *31*, 431–446.
117. Feixas, F.; Matito, E.; Poater, J.; Solà, M. Aromaticity of Distorted Benzene Rings. Exploring the Validity of Different Indicators of Aromaticity. *J. Phys. Chem. A* **2007**, *111*, 4513–4521.
118. Feixas, F.; Jiménez-Halla, J.O.C.; Matito, E.; Poater, J.; Solà, M. A Test to Evaluate the Performance of Aromaticity Descriptors in All-Metal and Semimetal Clusters. An Appraisal of Electronic and Magnetic Indicators of Aromaticity. *J. Chem. Theory Comput.* **2010**, *6*, 1118–1130.
119. Nigam, S.; Majumder, C.; Kulshreshtha, S.K. Structure and Bonding of Tetramer Clusters: Theoretical Understanding of the Aromaticity. *J. Mol. Struct. (Theochem)* **2005**, *755*, 187–194.
120. Seal, P. Is Nucleus-Independent Chemical Shift Scan a Reliable Aromaticity Index for Planar and Neutral A_2B_2 Clusters? *J. Mol. Struct. (Theochem)* **2009**, *893*, 31–36.
121. Jusélius, J.; Straka, M.; Sundholm, D. Magnetic-Shielding Calculations on Al_4^{2-} and Analogues. A New Family of Aromatic Molecules? *J. Phys. Chem. A* **2001**, *105*, 9939–9944.
122. Santos, J.C.; Tiznado, W.; Contreras, R.; Fuentealba, P. Sigma-pi Separation of the Electron Localization Function and Aromaticity. *J. Chem. Phys.* **2004**, *120*, 1670–1673.
123. Fowler, P.W.; Havenith, R.W.A.; Steiner, E. Unconventional Ring Currents in an 'All-Metal Aromatic', Al_4^{2-}. *Chem. Phys. Lett.* **2001**, *342*, 85–90.
124. Fowler, P.W.; Havenith, R.W.A.; Steiner, E. Ring Current and Electron Delocalization in an All-Metal Cluster, Al_4^{2-}. *Chem. Phys. Lett.* **2002**, *359*, 530–536.
125. Zhai, H.-J.; Wang, L.-S.; Kuznetsov, A.E.; Boldyrev, A.I. Probing the Electronic Structure and Aromaticity of Pentapnictogen Cluster Anions Pn_5^- (Pn = P, As, Sb, and Bi). Using Photoelectron Spectroscopy and *ab Initio* Calculations. *J. Phys. Chem. A* **2002**, *106*, 5600–5606.
126. Jin, Q.; Jin, B.; Xu, W.G.; Zhu, W. Aromaticity of Planar P_5^- Anion in the P_5M (M = Li, Na, and K) Clusters. *J. Mol. Struct. (Theochem)* **2005**, *713*, 113–117.
127. Kraus, F.; Korber, N. The Chemical Bond in Polyphospides: Crystal Structures, the Electron Localization Function, and a New View of Aromaticity in P_4^{2-} and P_5^-. *Chem. Eur. J.* **2005**, *11*, 5945–5959.
128. De Proft, F.; Fowler, P.W.; Havenith, R.W.A.; Schleyer, P.v.R.; Van Lier, G.; Geerlings, P. Ring Currents as Probes of the Aromaticity of Inorganic Monocycles: P_5^-, As_5^-, S_2N_2, $S_3N_3^-$, $S_4N_3^+$, $S_4N_4^{2+}$, $S_5N_5^+$, S_4^{2+} and Se_4^{2+}. *Chem. Eur. J.* **2004**, *10*, 940–950.